EUROPEAN ORGANIZATION FOR NUCLEAR RESEARCH

L3 Note 2452
August 19, 1999

Search for Charged Higgs Bosons in e^+e^- Collisions at $\sqrt{s} = 189$ GeV

P. García–Abia, A. Kopp, Z. Szillasi

Abstract

A search for pair–produced charged Higgs bosons is performed with the L3 detector at LEP using data collected at a centre–of–mass energy of 188.6 GeV, corresponding to an integrated luminosity of 176.4 pb^{-1}. Higgs decays into a charm and a strange quark or into a tau lepton and its associated neutrino are considered. The observed events are consistent with the expectations from Standard Model background processes. A lower limit of 65.5 GeV on the charged Higgs mass is derived at 95% confidence level, independent of the decay branching ratio $Br(H^{\pm} \to \tau\nu)$.

To be submitted to *Phys. Lett. B*

Introduction

In the Standard Model [1], the Higgs mechanism [2] requires one doublet of complex scalar fields which leads to the prediction of a single neutral scalar Higgs boson. Extensions to the minimal Standard Model contain more than one Higgs doublet [3]. In particular, models with two complex Higgs doublets predict two charged Higgs bosons ($H^{\pm}$). The discovery of a charged Higgs particle would be evidence for physics beyond the Standard Model.

The search is performed in the three decay channels $H^+H^- \to \tau^+\nu_\tau\tau^-\bar{\nu}_\tau$, $H^+H^- \to c\bar{s}\tau^-\bar{\nu}_\tau$ [1)] and $H^+H^- \to c\bar{s}c\bar{s}$. This allows the interpretation of the results to be independent of the branching ratio $Br(H^{\pm} \to \tau\nu)$.

The results include and supersede the previous lower limit on the mass of charged Higgs bosons established by L3 [4, 5]. Results from other LEP experiments are published in Reference [6].

Data Analysis

This letter describes the search for pair–produced charged Higgs bosons using the data collected with the L3 detector [7] at LEP at $\sqrt{s} = 188.6$ GeV, corresponding to an integrated luminosity of 176.4 pb^{-1}. The analyses remain almost unchanged since our previous publication at centre–of–mass energies between 130 and 183 GeV [4], because they show a similar performance.

The charged Higgs cross section is calculated using the HZHA Monte Carlo program [8]. For the efficiency estimates, samples of $e^+e^- \to (Z/\gamma) \to H^+H^-$ events are generated with the PYTHIA Monte Carlo program [9] for Higgs masses between 50 and 90 GeV in mass steps of 5 GeV. About 1000 events for each final state are generated at each Higgs mass. For the background studies the following Monte Carlo generators are used: PYTHIA for $e^+e^- \to q\bar{q}(\gamma)$, $e^+e^- \to ZZ$ and $e^+e^- \to Ze^+e^-$, KORALW [10] for $e^+e^- \to W^+W^-$, PHOJET [11] for $e^+e^- \to e^+e^-q\bar{q}$, DIAG36 [12] for $e^+e^- \to e^+e^-\ell^+\ell^-$ ($\ell = e, \mu, \tau$), KORALZ [13] for $e^+e^- \to \mu^+\mu^-$ and $e^+e^- \to \tau^+\tau^-$ and BHAGENE3 [14] for $e^+e^- \to e^+e^-$. The L3 detector response is simulated using the GEANT program [15] which takes into account the effects of energy loss, multiple scattering and showering in the detector.

Search in the $H^+H^- \to \tau^+\nu_\tau\tau^-\bar{\nu}_\tau$ Channel

The signature for the leptonic decay channel is a pair of tau leptons with large missing energy and momentum, giving rise to low multiplicity events with low visible energy and uniform acollinearity, the maximum angle between any pair of tracks. This distribution is shown in Figure 1. The performance of the analysis is not affected by the increased centre–of–mass energy, and the event selection remains unchanged since our last publication [4].

The efficiency of the $H^+H^- \to \tau^+\nu_\tau\tau^-\bar{\nu}_\tau$ selection for several Higgs masses is shown in Table 1. The total number of events selected in data is 30, where 32.5 background events are expected from Standard Model processes. Almost all of the remaining background comes from W pair production.

[1)] The charge conjugate reaction is included throughout the letter.

Channel	Efficiency (%) for $m_{H^\pm}$ =					Background	DATA
	60 GeV	65 GeV	70 GeV	75 GeV	80 GeV		
$H^+H^- \to \tau^+\nu_\tau\tau^-\bar{\nu}_\tau$	24	27	31	32	34	32.5	30
$H^+H^- \to c\bar{s}\tau^-\bar{\nu}_\tau$	44	42	40	39	34	129.3	138
$H^+H^- \to c\bar{s}\bar{c}s$	39	38	38	34	30	359.4	348

Table 1: The charged Higgs efficiencies for various Higgs masses, the background expectations and the number of data events. The total error on the efficiency and on the background expectations is estimated to be 5% and 10%, respectively.

Search in the $H^+H^- \to c\bar{s}\tau^-\bar{\nu}_\tau$ Channel

The semileptonic final state $H^+H^- \to c\bar{s}\tau^-\bar{\nu}_\tau$ is characterised by two hadronic jets, a tau lepton and missing momentum. The selection criteria are slightly modified with respect to the analysis at lower centre–of–mass energies [4], in order to gain sensitivity at higher masses.

High multiplicity events are selected by requiring more than five charged tracks, more than 10 calorimetric clusters and a visible energy greater than $0.35\sqrt{s}$. The visible mass of the jet–jet system must be less than 110 GeV and the energy of the visible decay products of the tau lepton less than 50 GeV to reduce $q\bar{q}(\gamma)$ contamination. This background is further reduced by requiring the missing transverse momentum to exceed 25 GeV, the missing momentum parallel to the beam axis to be less than 50% of the visible energy and the direction of the missing momentum vector to satisfy $|\cos\theta_{\rm miss}| < 0.9$. The sum of the opening angles of the tau candidate and the missing momentum vector to the closest jet must be larger than 70°. Semileptonic decays of W pairs in electrons or muons are suppressed requiring the sum $E^*_\ell + |P^*_{\rm miss}|$ to be less than 60 GeV for an electron and less than 50 GeV for a muon in the final state, where E^*_ℓ and $P^*_{\rm miss}$ are the energy of the lepton and the missing momentum in the rest frame of the parent particle, respectively. The distribution of $E^*_\ell + |P^*_{\rm miss}|$ is shown in Figure 2a. Contamination from $q\bar{q}$ (γ), two–photon interactions and W pair events is further reduced by requiring $|\cos\Theta| \leq 0.9$, where Θ is the polar angle of the parent particle.

The gain in efficiency with these cuts relative to the analysis at lower centre–of–mass energies is 30% for a Higgs of 80 GeV mass. The selection efficiencies are shown in Table 1. The total number of events selected in data is 138, where 129.3 background events are expected from Standard Model processes. The background is dominated by the process $W^+W^- \to q\bar{q}'\tau\nu$. Figure 2b shows the average of the masses of the jet–jet and the τ–ν systems, calculated after a kinematic fit imposing energy and momentum conservation for an assumed production of a pair of equal mass particles.

Search in the $H^+H^- \to c\bar{s}\bar{c}s$ Channel

Events from the $H^+H^- \to c\bar{s}\bar{c}s$ channel have a high multiplicity and are balanced in transverse and longitudinal momenta. A large fraction of the centre–of–mass energy is deposited in the detector, typically by four hadronic jets. The performance of the analysis is unchanged with respect to our previous analysis [4], hence the same set of selection cuts is used.

The selection efficiencies are shown in Table 1. The total number of events selected in data is 348, where 359.4 background events are expected from Standard Model processes. The main contribution to the background comes from W pair decays into four jets. Figure 3 shows the average dijet mass after a kinematic fit imposing four–momentum conservation and equal dijet

masses. The low mass tail from the W^+W^- background is due to incorrectly assigned jet pairs.

Results

The number of selected events in each decay channel is consistent with the number of events expected from Standard Model processes, and no significant deviations in the mass spectra are present. No indication of pair–produced charged Higgs bosons is observed. Mass limits as a function of the branching fraction $\mathrm{Br}(H^\pm \to \tau\nu)$ are derived at the 95% confidence level (CL), using the same technique described in Reference [16]. For the $H^+H^- \to c\bar{s}\bar{c}s$ and the $H^+H^- \to c\bar{s}\tau^-\bar{\nu}_\tau$ channels the reconstructed mass distributions (Figures 2b and 3) are used in the limit calculation, whereas for the $H^+H^- \to \tau^+\nu_\tau\tau^-\bar{\nu}_\tau$ channel the total number of data, expected background and expected signal events are used.

The systematic uncertainties on the background and signal are estimated to be 10% and 5% [17] respectively, and come mainly from normalisation errors due to selection efficiencies and cross sections. These errors are included in the confidence level calculation.

Figure 4 shows the excluded mass regions of charged Higgs bosons at 95% CL for the analyses of each final state and their combination as function of the branching fraction $\mathrm{Br}(H^\pm \to \tau\nu)$, including the data from $\sqrt{s} = 188.6$ GeV as well as those from lower centre–of–mass energies. The region around $m_{H^\pm} = 67$ GeV at low values of $\mathrm{Br}(H^\pm \to \tau\nu)$ can only be excluded at 88% CL, due to the slight excess in data in this mass region (Figure 3). For a branching fraction of $\mathrm{Br}(H^\pm \to \tau\nu) > 0.2$, the 95% CL lower limit on the charged Higgs mass is 71.6 GeV.

The limit reveals a significant improvement on the sensitivity of the data as compared to that from lower centre–of–mass energies. A lower limit on the mass of the charged Higgs boson of

$$m_{H^\pm} > 65.5 \text{ GeV}$$

independent of the branching fraction is obtained.

Acknowledgements

We wish to express our gratitude to the CERN accelerator divisions for the excellent performance of the LEP machine. We acknowledge the efforts of engineers and technicians who have participated in the construction and maintenance of the experiment.

References

[1] S.L. Glashow, Nucl. Phys. **22** (1961) 579;
S. Weinberg, Phys. Rev. Lett. **19** (1967) 1264;
A. Salam, "Elementary Particle Theory", edited by N. Svartholm (Almqvist and Wiksell, Stockholm, 1968), p. 367.

[2] P.W. Higgs, Phys. Lett. **12** (1964) 132, Phys. Rev. Lett. **13** (1964) 508 and Phys. Rev. **145** (1966) 1156;
F. Englert and R. Brout, Phys. Rev. Lett. **13** (1964) 321;
G.S. Guralnik, C.R. Hagen and T.W.B. Kibble, Phys. Rev. Lett. **13** (1964) 585.

[3] S. Dawson *et al.*, The Physics of the Higgs Bosons: Higgs Hunter's Guide, Addison Wesley, Menlo Park, 1989.

[4] L3 Collab., M. Acciarri *et al.*, Phys. Lett. **B 446** (1999) 368.

[5] L3 Collab., O. Adriani *et al.*, Phys. Lett. **B 294** (1992) 457;
L3 Collab., O. Adriani *et al.*, Z. Phys. **C 57** (1993) 355.

[6] ALEPH Collab., R. Barate *et al.*, Phys. Lett. **B 418** (1998) 419;
ALEPH Collab., R. Barate *et al.*, Phys. Lett. **B 450** (1999) 467;
DELPHI Collab., P. Abreu *et al.*, Phys. Lett. **B 420** (1998) 140;
OPAL Collab., K. Ackerstaff *et al.*, Phys. Lett. **B 426** (1998) 180;
OPAL Collab., G. Abbiendi *et al.*, Eur. Phys. J. **C 7** (1999) 407.

[7] L3 Collab., B. Adeva *et al.*, Nucl. Instr. Meth. **A 289** (1990) 35;
J.A. Bakken *et al.*, Nucl. Instr. Meth. **A 275** (1989) 81;
O. Adriani *et al.*, Nucl. Instr. Meth. **A 302** (1991) 53;
B. Adeva *et al.*, Nucl. Instr. Meth. **A 323** (1992) 109;
K. Deiters *et al.*, Nucl. Instr. Meth. **A 323** (1992) 162;
M. Chemarin *et al.*, Nucl. Instr. Meth. **A 349** (1994) 345;
M. Acciarri *et al.*, Nucl. Instr. Meth. **A 351** (1994) 300;
G. Basti *et al.*, Nucl. Instr. Meth. **A 374** (1996) 293;
A. Adam *et al.*, Nucl. Instr. Meth. **A 383** (1996) 342.

[8] P. Janot, in Physics at LEP2, ed. G. Altarelli, T. Sjöstrand and F. Zwirner, (CERN 96-01, 1996), volume 2, p. 309.

[9] T. Sjöstrand, CERN-TH 7112/93, CERN (1993), revised August 1995;
T. Sjöstrand, Comp. Phys. Comm. **82** (1994) 74.

[10] M. Skrzypek *et al.*, Comp. Phys. Comm. **94** (1996) 216;
M. Skrzypek *et al.*, Phys. Lett. **B 372** (1996) 289.

[11] R. Engel, Z. Phys. **C 66** (1995) 203;
R. Engel and J. Ranft, Phys. Rev. **D 54** (1996) 4244.

[12] F.A. Berends, P.H. Daverfeldt and R. Kleiss, Nucl. Phys. **B 253** (1985) 441.

[13] S. Jadach, B.F.L. Ward and Z. Wąs, Comp. Phys. Comm. **79** (1994) 503.

[14] J.H. Field, Phys. Lett. **B 323** (1994) 432;
J.H. Field and T. Riemann, Comp. Phys. Comm. **94** (1996) 53.

[15] R. Brun *et al.*, "GEANT 3", CERN DD/EE/84-1 (Revised), September 1987.
The GHEISHA program (H. Fesefeldt, RWTH Aachen Report PITHA 85/02, 1985) is used to simulate hadronic interactions.

[16] L3 Collab., M. Acciarri *et al.*, Phys. Lett. **B 411** (1997) 373.

[17] L3 Collab., M. Acciarri *et al.*, CERN-PPE/99-80, to be published in Phys. Lett. B.

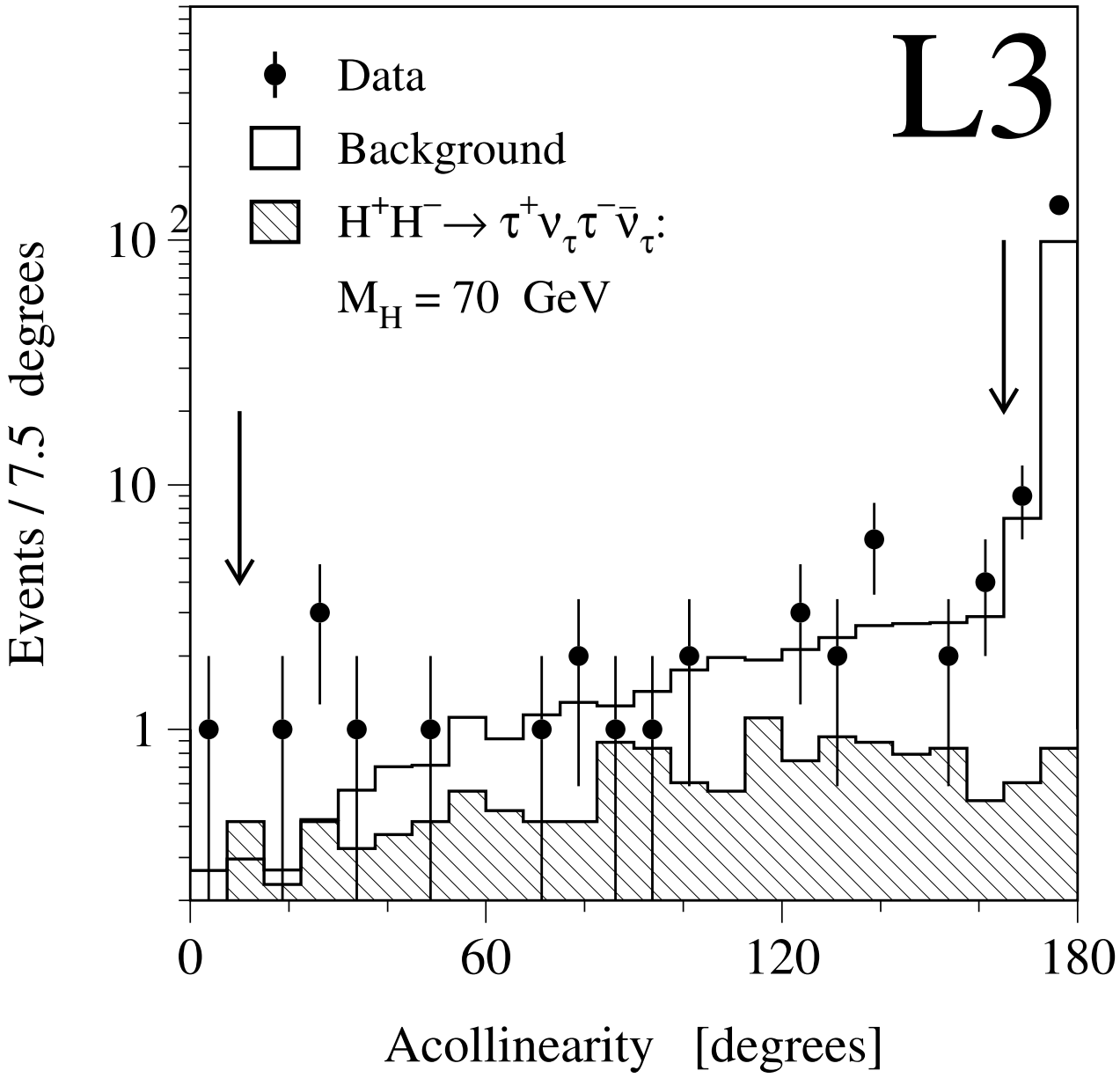

Figure 1: The maximum angle between any pair of tracks, or acollinearity, for the $H^+H^- \to \tau^+\nu_\tau\tau^-\bar{\nu}_\tau$ channel after all other cuts have been applied. The arrows show the position of the cut. The hatched histogram indicates the expected distribution for a 70 GeV Higgs at $\mathrm{Br}(H^\pm \to \tau\nu) = 1$.

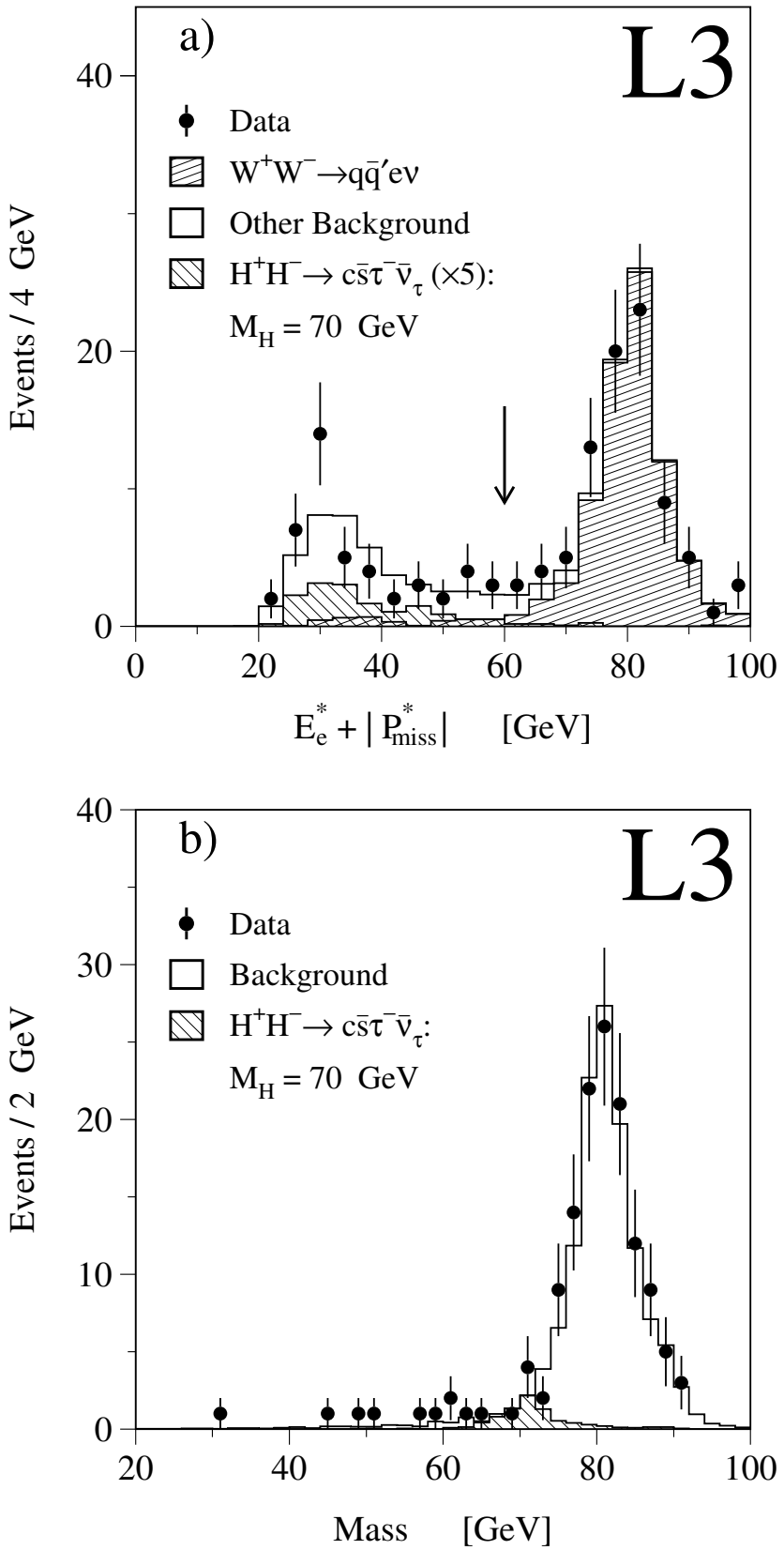

Figure 2: Distributions for the $H^+H^- \to c\bar{s}\tau^-\bar{\nu}_\tau$ channel. a) $E_e^* + |P_{miss}^*|$ for events with an identified electron in the final state after all other cuts, the arrow indicates the position of the cut. b) Reconstructed mass spectrum after all cuts. The expected distribution for a 70 GeV Higgs at $Br(H^\pm \to \tau\nu) = 0.5$ is superimposed, multiplied by a factor five in a).

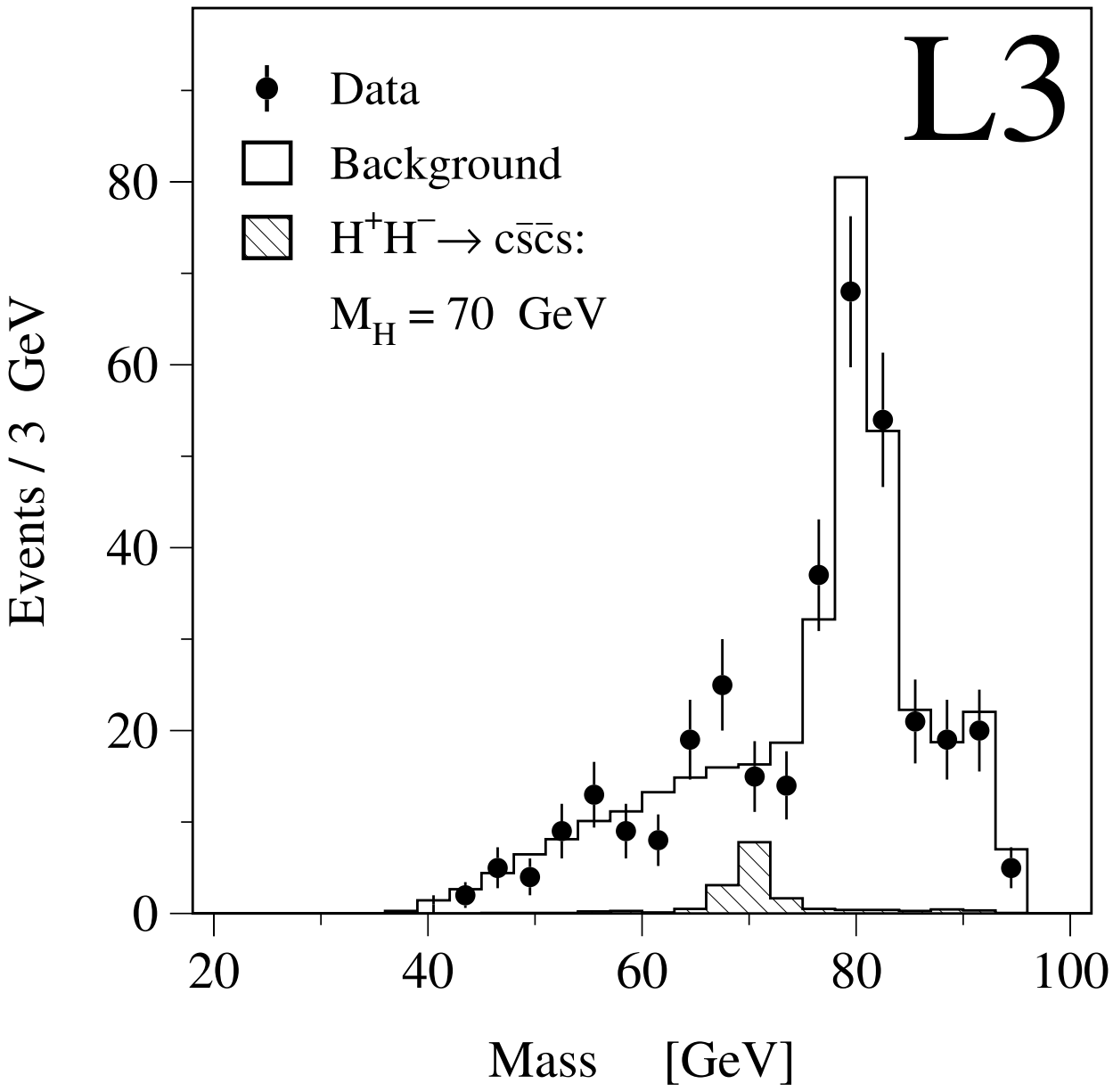

Figure 3: Distribution of the mass resulting from a kinematic fit, with assumed production of a pair of equal mass particles, for data and background events in the $H^+H^- \rightarrow c\bar{s}\bar{c}s$ channel. The hatched histogram indicates the expected distribution for a 70 GeV Higgs at $Br(H^\pm \rightarrow \tau\nu) = 0$.

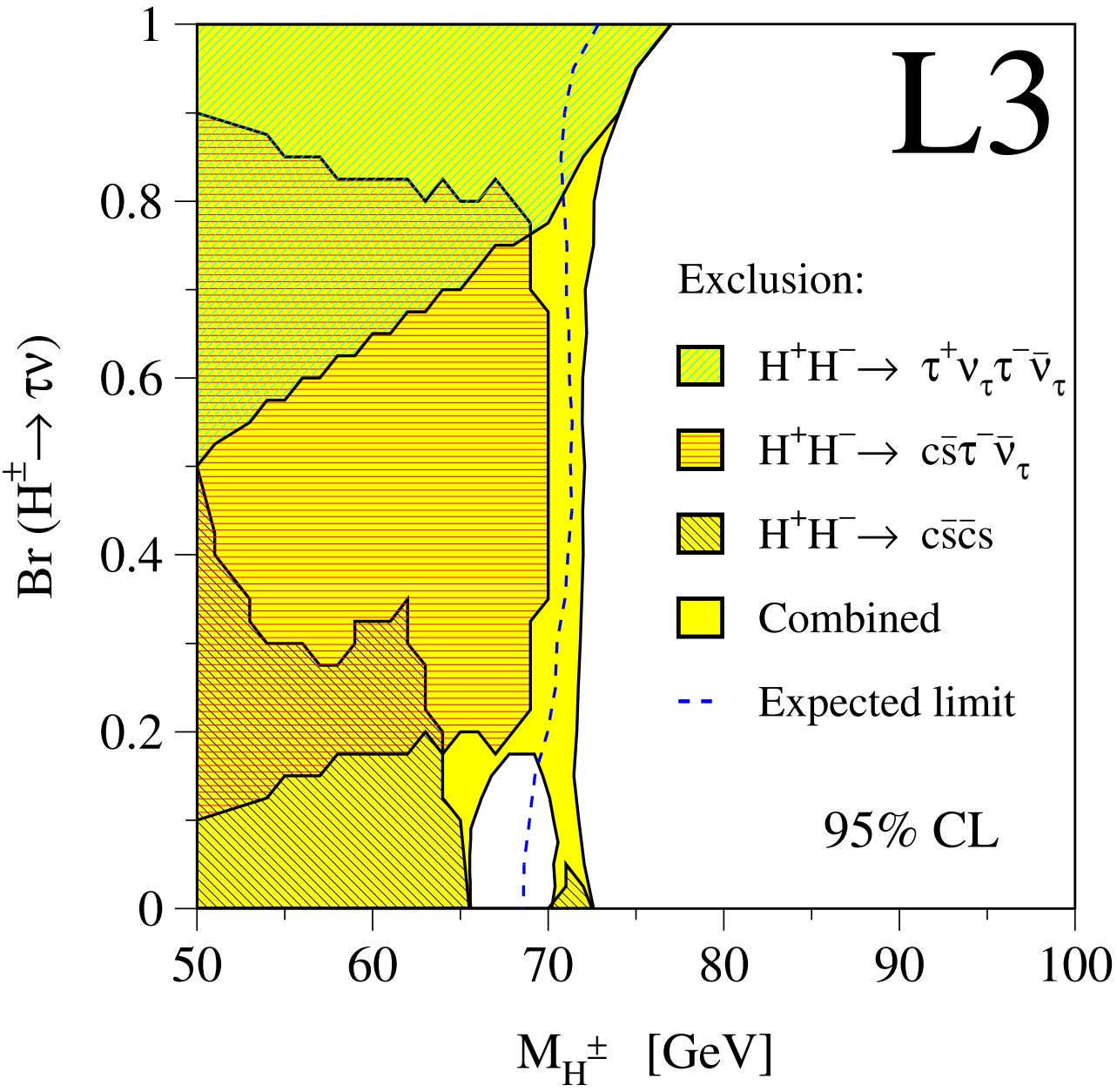

Figure 4: Excluded regions for the charged Higgs boson at 95% CL in the plane of the branching fraction $\mathrm{Br}(\mathrm{H}^\pm \to \tau\nu)$ versus mass. The dashed line indicates the median expected exclusion in the absence of a signal.